Discriminative temperature dependencies of differential light-scattering cross sections from an electron gas in semiconductors with a nonparabolic dispersion of energy bands

B. H. Bairamov,* V. A. Voitenko, I. P. Ipatova, V. K. Negoduyko, and V. V. Toporov
A. F. Ioffe Physico-Technical Institute, Russian Academy of Sciences, St. Petersburg, 194021, Russia
(Received 24 May 1994)

We present the results of a direct comparison between experiment and theory of the temperature dependencies of the integrated intensities and spectral linewidths in the quasielastic light-scattering spectra from the electron gas in III-V semiconductors. An explicit expression for the inelastic-electronic light-scattering cross sections in semiconductors with nonparabolic dispersion of energy bands is given for a realistic hydrodynamic free-electron-gas model. We find rather different effects of single-particle electronic excitations on polarized and depolarized scattering in n-InP in the temperature range 27–300 K with near infrared excitation of the spectra. The results provide clear evidence for the existence of strong temperature-dependent free-electron-gas fluctuations and prove unambiguously the observation of light scattering from energy- and momentum-density fluctuations.

I. INTRODUCTION

One of the most important subjects of semiconductor physics remains the many-body properties of the electron gas and inelastic light scattering by electronic excitations which is of strong current interest and is a fast developing branch of optical spectroscopy. In particular, the papers concerning the electronic light scattering cover one of the most exciting chapters in the optics of microstructures and superlattices.[1]

In spite of the considerable distinction between electronic properties of solids (metals, semiconductors, semimetals, and superconductors) there is an obvious resemblance in their light-scattering spectra. A common feature of all the types of electronic Raman-scattering (RS) processes comes from conservation laws, which govern them and make the energy $\hbar\omega$, and the momentum $\hbar q$, transferred during the scattering process, small. Within the framework of the effective-mass approximation the light-scattering mechanisms in semiconductor quantum wells and superlattices are similar to those of the parent three-dimensional (3D) systems.[1,2]

These are all conditions for observation of the majority of known single-particle excitations by the RS technique in III-V semiconductors. These excitations form the basic mechanisms of scattering which include charge-density fluctuations,[3] energy- and momentum-density fluctuations[4] as well as spin-density fluctuations.[5,6]

Scattering from charge-density fluctuations are well known from classical atomic plasmas. Scattering from energy-density and momentum-density fluctuations was first proposed by Wolf[4] and is based on deviations from parabolic behavior which exist for electronic bands of III-V compounds.

The most effective mechanism of light scattering from spin-density fluctuations comes from spin-orbit interactions. Such scattering has been observed in depolarized spectra (when polarizations of the incident and scattered light are orthogonal) of direct-gap bulk semiconductors such as GaAs,[7] InSb,[8] InP,[9] CdTe,[10] as well as of lower-dimensional structures such as heterostructures and quantum wells—an especially active field [see Ref. 11 for a review and recent reports (Refs. 12–16)].

In polarized spectra (the two polarizations are parallel to each other) light scattering from energy-density fluctuations was first observed by Mooradian[7] and from momentum-density fluctuations by Pinczuk *et al.* and can be found in the spectrum shown in Ref. 17. In the later work, it was, namely, momentum-density rather than energy-density fluctuations that scatter the light, because scattering occurred at a rather low temperature $T=10$ K. Light scattering from energy-density fluctuations was explored once again by Abramson, Tsen, and Brey[18] at room temperature.

All of these works are concerned with the bulk crystals. But RS from energy-density fluctuations is also clearly seen in 2D electron systems. It has been observed by Pinczuk *et al.* and can be found in polarized spectra shown in Fig. 4.12. from Ref. 2 and Fig. 1.8. from Ref. 19. This is not surprising since the nonparabolicity of the electronic energy bands is highly enhanced in quantum wells by interface states.[20]

Nevertheless, there has been considerable controversy concerning the origin of electronic scattering from single-particle excitations. While the details of depolarized scattering are generally well known,[12,17] the exact mechanisms for polarized scattering still remain unresolved. Polarized spectra are usually interpreted as arising from charge-density excitations. Recently, Cardona and Ipatova[21] have pointed out that it is necessary to find additional quantitative comparison between predicted and measured absolute scattering efficiencies from energy- and momentum-density fluctuations in order to lift uncertainty concerning the efficiency of the scattering.

Most of the recent inelastic electronic light-scattering experiments have been carried out in GaAs with excitation photon energies $\hbar\omega_i$ in the range 1.5–1.9 eV close to the resonance with fundamental E_0, spin-orbit split-off $E_0+\Delta_0$ optical gaps, or with quantum-well excitons pro-

viding the large scattering enhancement required for sufficient sensitivity. On the other hand, the simultaneous appearance of a strong hot luminescence in such cases allows one to carry out measurements only in a limited electron concentration range and prevents temperature-dependent measurements which, as we will show below, are essential for the observation of new features in the light-scattering spectra from electronic excitations in semiconductors.

In this paper, we examine the different scattering mechanisms from electronic excitations by using nonresonant near-infrared excitation of n-InP: $E_g+\Delta_0=1.43+0.11=1.54$ eV (at $T=10$ K) and $\hbar\omega_i=1.17$ eV. The absence of an intense background hot luminescence in this case has provided us with an opportunity to carry out not only the conventional polarization studies but also temperature-dependent measurements of the integrated intensities and spectral linewidths of the quasielastic electronic-scattering spectra. We find rather different effects of electronic excitations on polarized and depolarized scattering and undertake both theoretical and experimental comparison between intensities of scattering from energy- and spin-density fluctuations. We find this approximately equal at room temperature which removes any possible doubts concerning scattering from energy-density fluctuations, since scattering from spin-density fluctuations is well established.

II. EXPERIMENTAL SETUP

Our polarized quasielastic scattering measurements were performed by using the 1064.2 nm line of a cw Nd^{3+}:YAG laser and doped n-InP sample in the temperature range 27–300 K. The temperature stability was

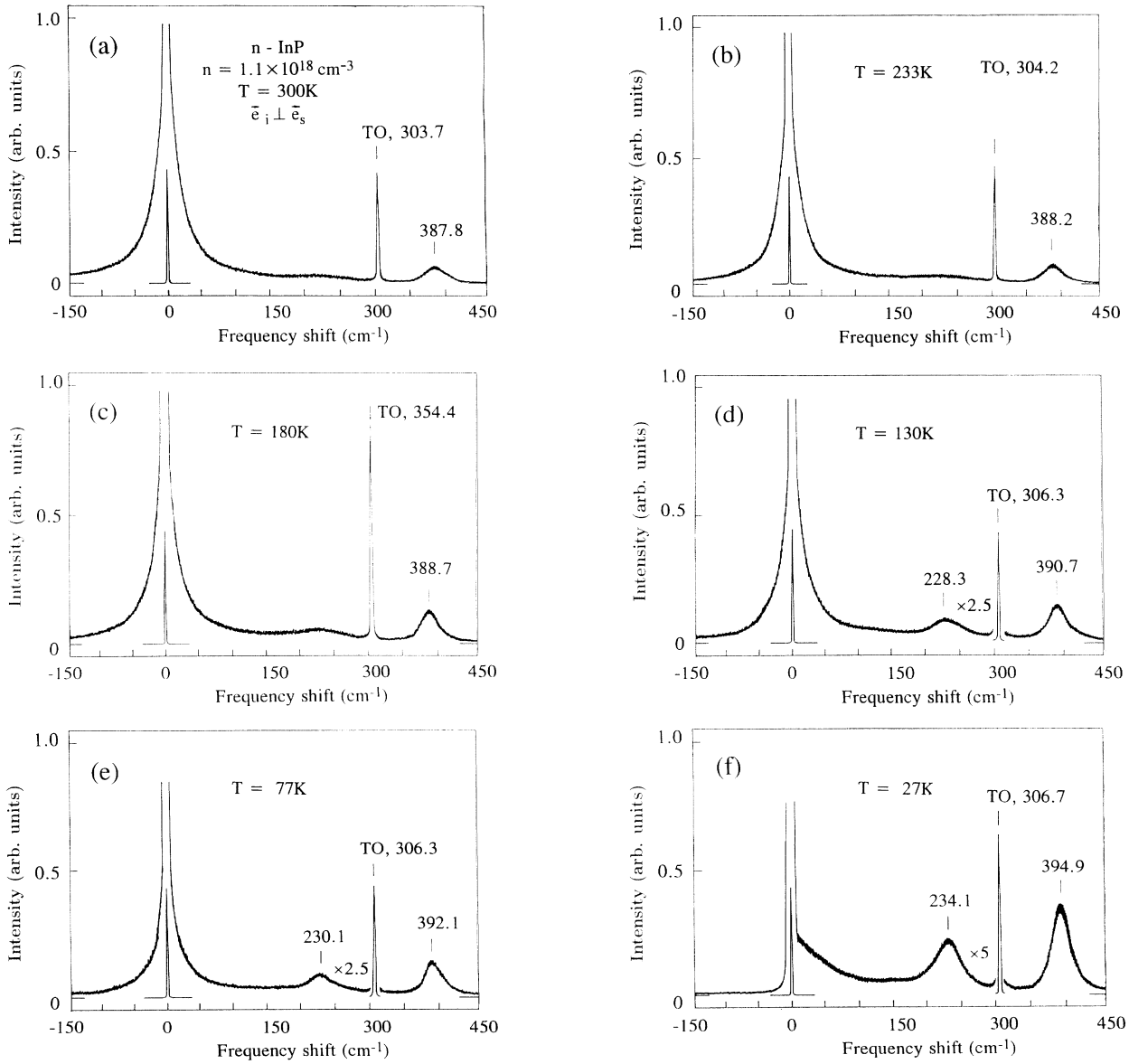

FIG. 1. (a)–(f) Experimental Raman spectra of n-InP sample with $n=1.1\times10^{18}$ cm^{-3} for crossed polarizations $\mathbf{e}_i\perp\mathbf{e}_s$ at different temperatures which are indicated in the figures. Quasielastic Lorentzian contours correspond to spin-density fluctuations.

typically ±1 K. We used intentionally doped high-quality homogeneous single crystals oriented along $(11\bar{2})$, $(\bar{1}10)$, and $(\bar{1}11)$ directions. The free-electron concentration $n=1.10\times10^{18}$ cm^{-3} (at $T=300$ K) was determined by Hall measurements and independently from Raman scattering by coupled plasmon-LO-phonon modes.[22] All measurements were conducted in a right-angle scattering geometry with the incident light always being along $(11\bar{2})$ and scattered light along $(\bar{1}11)$ directions: $(11\bar{2})\{(\bar{1}10),(\bar{1}10)\}(\bar{1}11)$ for polarized spectra, further labeled by $\bar{e}_i\|\bar{e}_s$ and $(11\bar{2})\{(\bar{1}10),(11\bar{2})\}(\bar{1}11)$ for depolarized spectra further labeled as $\bar{e}_i\perp\bar{e}_s$. The scattered light was analyzed by a double monochromator with a spectral resolution of 2.1 cm^{-1} and detected with a cooled photomultiplier tube with photon-counting electronic system.

To avoid sample heating effects[23] the laser power was maintained at a sufficiently low level of less than 20 mW, which we found was insufficient to affect the detected spectra. At each measured temperature we monitored the position of the sharp TO-phonon line and no detectable shifts were observed within the accuracy of better than ±0.05 cm^{-1} (by using Ne spectral lines for frequency calibration).

III. EXPERIMENTAL RESULTS

Figures 1(a)–1(f) show typical Raman spectra obtained from our n-InP sample in the frequency range from −150 up to 450 cm^{-1} and at different temperatures from 300 to 27 K for depolarized scattering configuration $(\bar{e}_i\perp\bar{e}_s)$. Figures 2(a)–2(f) show the same for polarized scattering configuration $(\bar{e}_i\|\bar{e}_s)$. The scan is linear in wavelength and the positions of the lines are indicated in

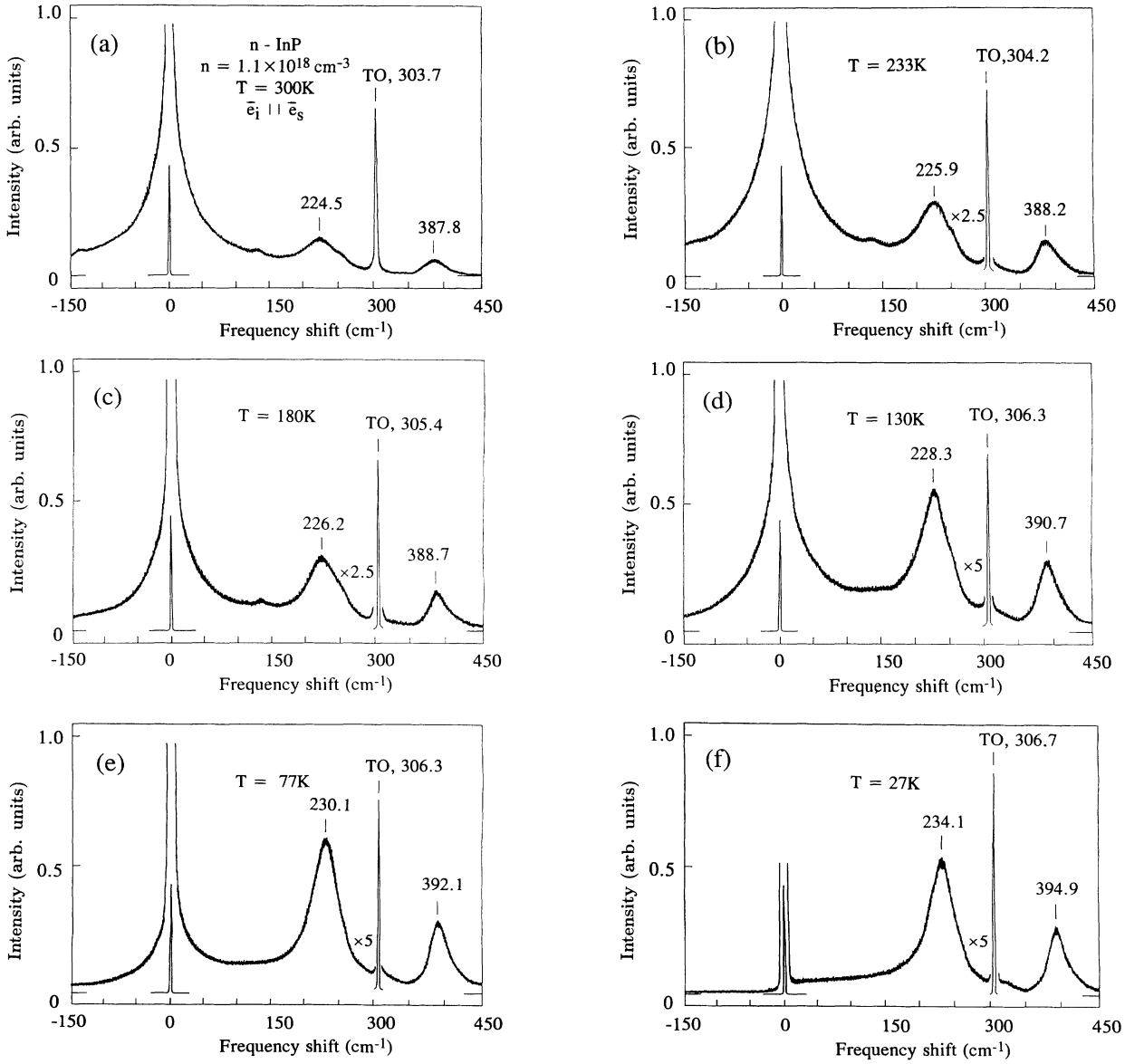

FIG. 2. The same as in (a)–(f) for scalar $\mathbf{e}_I\|\mathbf{e}_s$ scattering configuration. Quasielastic Lorentzian contours discussed in the text are near the laser line.

wave numbers.

We first consider the sharp narrow peaks observed in all spectra. They are due to the scattering by zone-center transverse optical TO (Γ) phonon. For the deconvoluted (corrected for instrumental resolution) intrinsic linewidth of this phonon line, we obtain 2.2 cm^{-1} at $T=300$ K. Both the linewidth and frequency of this phonon are not affected by the presence of a free-electron gas and are exactly the same as in semi-insulating InP with $n=1.0\times10^{9}$ cm^{-3}. The frequency of the TO (Γ)-phonon shifts with decreasing temperature from 303.7 cm^{-1}, which is exactly equal to that in semi-insulating InP at 300 K,[22] up to 306.7 cm^{-1} at $T=27$ K. This shift as well as the temperature dependence of the intensity of the TO (Γ)-phonon line, which is proportional to $(n+1)$, where $n=[\exp\hbar\omega_{TO(\Gamma)/2}/k_BT-1]^{-1}$ is the Bose-Einstein phonon occupation factor, is typical for first-order Raman scattering, if one takes into account cubic anharmonicity.[24]

In addition to the uncoupled TO (Γ)-phonon line, broad peaks of coupled low- and high-frequency plasmon LO (Γ) phonon are also clearly seen at 224.5 and 387.8 cm^{-1} (at $T=300$ K), respectively. Their frequencies are in good agreement with calculations based on deformation potential together with Frölich (electro-optic) or electric-field interaction mechanism by consideration of both effects of lattice and plasma damping of free-electron gas as well as nonparabolicity of conduction band.[25] The weak structure at 136 cm^{-1} detectable in the spectra taken at 300, 233, and 180 K is due to overton scattering by transverse acoustical phonons at X point of Brillouin zone. The shoulder at 252 cm^{-1} comes from scattering by acoustical combination of longitudinal and transverse phonons at K point. They are clearly identified in the second-order Raman-scattering spectra obtained for semi-insulating InP.[26] [The LO(Γ)-phonon frequency in undoped InP is 345.6 cm^{-1} at 300 K].

In our n-InP doped with shallow Si donors with $n=1.0\times10^{18}$ cm^{-3} (at $T=300$ K) due to overlap of impurity band with conduction band, the concentration and mobility of free-electron gas are almost temperature independent. And this behavior is reflected in observed small temperature dependencies of the low- and high-frequency plasmon-LO(Γ)-phonon bands. Finally, we unambiguously identify in all the spectra, sharp quasielastic parts of Raman scattering from free-electron gas located within ±150 cm^{-1} with the required characteristic finite intensity at frequencies close to zero. The Stokes and anti-Stokes components at near room temperatures are equal in intensity due to response of the detector and spectrometer used.

First of all, we find that the intensities of electronic quasielastic scattering at each measured temperature increases linearly with the excitation laser power, while for the frequencies of the low- and high-frequency plasmon-LO(Γ)-phonon bands under the same conditions, no shifts are observed. This is a strong indication that observed quasielastic scattering is caused by electrons which are already present in conduction band, rather than being photoexcited from shallow levels.

In order to determine the integrated values of the intensities of the quasielastic electronic scattering we used unoccupied TO(Γ)-phonon spectra for calibration, so that the spectra at different temperatures may be directly compared. So it is easily observed that the intensity as well as linewidth of quasielastic electronic scattering spectra considerably decreases with temperature. Figures 3 and 4 compare the corresponding experimental in-

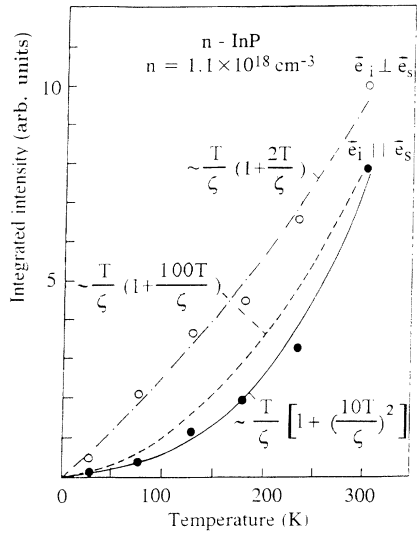

FIG. 3. Temperature dependence of the integrated cross section from the same sample as in Figs. 1 and 2(a)–2(f). Solid and dashed lines—theory for energy—momentum-density fluctuations corresponding to Eqs. (20) and (34), filled circles correspond to experimental points available for polarized scattering configuration from (a)–f. Dash-dotted line—theory for spin-density fluctuations [Eq. (29)], open circles correspond to experimental points available for depolarized scattering configuration from Figs. 1(a)–1(f).

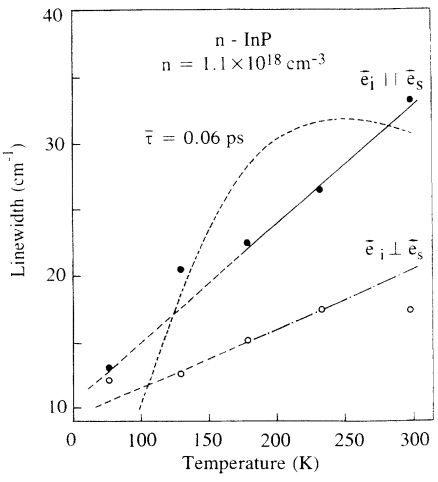

FIG. 4. Temperature dependence of the spectral linewidth Γ for the same sample as in Figs. 1–3. Scattering from energy-density fluctuations—upper straight line and dash-dotted curve (theory), filled circles—experiment. Scattering from spin-density fluctuations—lower straight line (theory) and open circles—experiment. Dashed parts of the lines belong to the region of degenerate statistics which is outside of framework of Eqs. (39) and (41).

tegrated intensities and linewidths. It is particularly striking, that a pronounced difference in the temperature dependencies of the intensity, as well as the linewidth of quasielastic electronic scattering between polarized and depolarized scattering configurations is readily observable.

IV. HYDRODYNAMIC FREE-ELECTRON-GAS MODEL AND THEORY OF QUASIELASTIC LIGHT SCATTERING

A. Mechanisms of scattering

It was recognized in the experimental work[27] concerned with light scattering n-Si in that momentum conservation within the elementary act of scattering is violated and the scattering process should be treated taking into account electron impurity collisions. Therefore the hydrodynamic model of electron gas is useful. It enables one to express the differential scattering cross section in terms of the correlation function of the electron susceptibility fluctuations $\delta\chi_{ij}(r,t)$,[28]

$$\frac{d^2\Sigma}{d\omega\, d\Omega}=\frac{1}{2\pi}\left[\frac{\omega_I^4}{c}\right]e_K^I e_j^s (e_i^I e_n^s)^* \times\int dt\int d^3r e^{i(\mathbf{qr}-\omega t)}\langle\delta\chi_{ij}(r,t)\delta\chi_{Kn}(0,0)\rangle\ , \tag{1}$$

where ω_I is the frequency of the incident light, $\bar{e}_I$ and $\bar{e}_s$ are the polarization vectors of the incident and scattered light, $\omega=\omega_I-\omega_s$ and q being the energy and the momentum transferred during the RS process, the angular brackets denote statistical averaging over the initial states of a crystal.

Symmetry arguments allow separation in the cross section (1) three independent contributions corresponding to the scalar $\frac{1}{3}\mathrm{Tr}\delta\chi$, symmetry

$$\delta\chi_{iK}^{(s)}=\tfrac{1}{2}(\delta\chi_{iK}+\delta\chi_{Ki}-\tfrac{2}{3}\mathrm{Tr}\delta\chi\delta_{iK}) \tag{2}$$

and antisymmetric

$$\delta\chi_{iK}^{(a)}=\tfrac{1}{2}(\delta\chi_{iK}-\delta\chi_{Ki}) \tag{3}$$

parts of electronic susceptibility.

The correlation function $(\delta\chi_{ij}\delta\chi_{Kn})q\omega$ from Eq. (1) reduces in the case of isotropic medium to the equation [see Eq. (117.13) from Ref. 28].

$$(\delta\chi_{ij}\delta\chi_{Kn})q\omega=(\tfrac{1}{3}\mathrm{Tr}\delta\chi)^2 q\omega\delta_{ij}\delta_{Kn} +\tfrac{1}{10}(\delta\chi^s)^2 q\omega(\delta_{iK}\delta_{jn}+\delta_{in}\delta_{Kj}-\tfrac{2}{3}\delta_{ij}\delta_{Kn}) +\tfrac{1}{6}(\delta\chi^a)^2 q\omega(\delta_{iK}\delta_{jn}-\delta_{in}\delta_{Kj})\ . \tag{4}$$

Here, in the standard notations of the textbook[28] $(\cdots)^2 q\omega$ denotes the Fourier transform in time and space of the correlation function entering the cross section (1). Three terms on the right-hand side of Eq. (4) represent the three different mechanisms of light scattering.

The scalar contribution into the correlation function (4) includes charge-density and energy-density fluctuations. They have the same (scalar) symmetry and are not statistically independent. Coupling of them is treated in Ref. 29. When the heavy screening condition holds

$$qr_s \ll 1\ , \tag{5}$$

where r_s is the screening length, the charge-density fluctuations lead to RS from plasmon-phonon modes which is realized in the region of higher frequencies

$$\omega\sim\omega_p \gg \tau^{-1}\ . \tag{6}$$

ω_p being the plasma frequency, τ is the electron relaxation time. It is not considered here.

Energy-density fluctuation δE gives rise to RS due to nonparabolicity of electronic band structure.[4] Corresponding contribution to $\delta\chi$ is proportional to the fluctuation δE of the electron kinetic energy

$$\delta\chi^{\varepsilon}=\frac{e^2}{m\omega_I^2}B_{\varepsilon}(\omega_I)\delta E\ , \tag{7}$$

where in the two-band approximation, see, e.g., Ref. 30,

$$B_{\varepsilon}(\omega_I)=\frac{2P_{cv}^2}{3m}\sum_j\frac{E_{gj}^2+(\hbar\omega_I)^2}{[E_{gj}^2-(\hbar\omega_I)^2]^2}\left[1+\frac{m_e^*}{m_j^*}\right]\ , \tag{8}$$

$$\delta E=\int\frac{2d^3p}{(2\pi\hbar)^3}\frac{p^2}{2m_e^*}\delta f_p^{(1)}\ , \tag{9}$$

P_{cv} being the interband momentum matrix element, $\delta f_p^{(1)}$—the spherically symmetric fluctuation of the electron distribution function, and m_j^*—the effective mass of the heavy holes ($j=1$), light holes ($j=2$), and the spin-orbit split-off band ($j=3$). Further, we settle $E_{g1}=E_{g2}=E_g$, $E_{g3}=E_g+\Delta$, Δ being the spin-orbit splitting of the valence band in the Γ point of Brilloiun zone. The scattering cross section corresponding to Eq. (7) is observed in parallel polarizations $e_I\|e_s$.

The symmetric contribution into the correlation function (4) is also caused by nonparabolicity of electronic energy spectrum.[4] It should contribute to light scattering from momentum-density fluctuations. It is seen from Eq. (4) that this scattering is statistically independent from scattering by charge-density fluctuations and therefore is not screened. Appropriate contribution to the fluctuation of the electron susceptibility in case of weak nonparabolicity has the form[30]

$$\delta\chi^s=-\frac{e^2}{m\omega_I^2}\int\frac{2d^3p}{(2\pi\hbar)^3}B_p(\omega_I)p_x p_y\delta f_p^{(2)}\ , \tag{10}$$

$$B_p(\omega_I)=\frac{2}{3}\frac{P_{cv}^4}{m^2E_g}\frac{E_g^2+(\hbar\omega_I)^2}{[E_g^2-(\hbar\omega_I)^2]^{2'}}\ , \tag{11}$$

P_x, P_y being Cartesian projections of electron momentum, $\delta f_p^{(2)}$ the anisotropic fluctuation of the electron distribution function. The scattering cross section corresponding to Eq. (1) is nonzero both in parallel and in perpendicular polarizations of the incident and scattered light.

The antisymmetric part of the tensor, $\delta\chi_{ij}$ is caused by the spin-density fluctuations.[5] It is equal to

$$\delta\chi^a = i\frac{e^2}{m\omega_I^2} B_\sigma(\delta n_\uparrow - \delta n_\downarrow) . \quad (12)$$

Here $\delta n_\uparrow - \delta n_\downarrow$ is the difference of the populations of the spin subbands and in the two-band approximation

$$B_\sigma(\omega_I) = \hbar\omega_I \frac{2P_{cv}^2}{3m} \frac{\Delta(\Delta+2E_g)}{[E_g^2-(\hbar\omega_I)^2][(E_g+\Delta)^2-(\hbar\omega_I)^2]} . \quad (13)$$

The light-scattering matrix elements (8), (11), and (13) are expressed through the same two-band parameters. That is why formulas (8), (11), and (13) enable one to estimate relative values of different RS cross sections and to reduce the problem of confirming them to the mechanism of spin-density fluctuations as most reliable. This procedure enables us to describe the light scattering in parallel polarizations (or so-called "polarized" light scattering) in terms of energy-momentum density fluctuations without measuring absolute scattering efficiencies.

B. Scattering cross section

It is seen from Eq. (1) that the light-scattering cross section is proportional to the Fourier transform in space and time of the susceptibility correlation function and the scattering spectrum reflects the hydrodynamical stage of fluctuation decay. This stage is described by Lorentzian-like correlation functions[31] and, therefore, scattering cross sections:

$$\frac{d^2\Sigma}{d\omega\, d\Omega} = I\frac{F(\omega)}{\omega^2+\Gamma^2}\Gamma . \quad (14)$$

The coefficient I has the dimensions of (length x frequency)$^{-1}$ and characterizes integrated cross section. It equals squared scattering amplitude (8), (11), or (13) multiplied by appropriate mean-square fluctuation. The constant represents the inverse time needed for fluctuation decay. Frequency dependent factor

$$F(\omega) = \frac{\hbar\omega}{1-e^{-\hbar\omega/T}} ,$$

provides the well-known Stokes to anti-Stokes ratio:

$$\frac{d\Sigma^{\text{Stokes}}}{d\Sigma^{\text{anti}}} = e^{\hbar\omega/T} .$$

Thus, in the case of energy-density fluctuations, we have

$$I_\varepsilon = \left[\frac{e^2}{mc^2}\right]^2 (\mathbf{e}_I\mathbf{e}_s)^2 B_\varepsilon^2(\omega_I)\langle\delta E^2\rangle . \quad (15)$$

The mean-square classical fluctuation of energy $\langle\delta E^2\rangle$ is determined by the temperature and by the heat capacity at constant volume C_v:[31]

$$\langle\delta E^2\rangle = C_v T^2 \quad (16)$$

provided fluctuations of electron concentration are negligible due to Eqs. (5,6). By substitution of Eq. (16) into (15), one gets

$$I_\varepsilon = \left[\frac{e^2}{mc^2}\right]^2 (\mathbf{e}_I\mathbf{e}_s)^2 B_\varepsilon^2(\omega_I) C_v T^2 . \quad (17)$$

It follows from Eq. (17) that the integrated RS cross section should decrease considerably with the lowering of temperature due to freezing out of energy fluctuations. This process is accelerated by the temperature dependence of the heat capacity C_v, which is sufficient when statistics become degenerate:

$$C_v = \frac{1}{T}\int \frac{2Vd^3p}{(2\pi\hbar)^3}\left[\frac{\delta f_0}{\delta\zeta}\right]_T\left[\varepsilon_p - \tfrac{3}{2}n\left[\frac{\delta\zeta}{\delta n}\right]_T\right]^2 , \quad (18)$$

where V is the crystal volume, f_0 is the Fermi distribution function and ζ is the chemical potential of the electrons.

It is pointed out in Ref. 30 that RS from momentum-density fluctuations is very weak with respect to the light scattering from the energy-density fluctuations. Appropriate small numerical factor $\frac{1}{10}$ emerges due to angular integration of the squared second Legandre polynomial which enters Eq. (10). Rigorous calculation undertaken in Refs. 32–34 leads to the equation

$$\frac{d\Sigma^E}{d\Sigma^p} = \left[\frac{10T}{\zeta}\right]^2 . \quad (19)$$

It follows from Eq. (19) that there is an opportunity to see light scattering from momentum-density fluctuations in experiment with the degenerate statistics of current carriers corresponding to low temperatures. In order to describe temperature dependence of the cross section in the case of parallel polarizations $e_I \| e_s$, one should take into account both contributions from energy and momentum-density fluctuations:

$$I_{\varepsilon,p} = \left[\frac{e^2}{mc^2}\right]^2 [\zeta B_p(\omega_I)]^2 \times V\left[\frac{\delta n}{\delta\zeta}\right]_T T\left[1+\left[\frac{10T}{\zeta}\right]^2\right] . \quad (20)$$

The effect of nonparabolicity is ruled out for crossed polarizations of incident and scattered light by the selection rules for energy and by the small factor $(\zeta B_p)^2 \ll 1$ for the momentum-density fluctuations.

One more contribution to the quasielastic scattering is determined according to Eq. (4) by the antisymmetric part of the electron-susceptibility tensor. It has the cross section

$$I_\sigma = V\left[\frac{e^2}{mc^2}B_\sigma(\omega_I)\right]^2 |\mathbf{e}_I\times\mathbf{e}_s^*|^2\langle(\delta n_\uparrow - \delta n_\downarrow)^2\rangle . \quad (21)$$

The mean-square fluctuation of the relative populations of the different spin subbands equals [see Ref. 31, part I, formula (115.2)].

$$\langle(\delta n_\downarrow - \delta n_\uparrow)^2\rangle = T\left[\frac{\delta n}{\delta\zeta}\right]_T , \quad (22)$$

where $n = n_\uparrow + n_\downarrow$ is the full population of the conduc-

tion band. It should be noted that in Eq. (21) the factor $T(\delta n/\delta\zeta)_T$ means the fraction of current carriers in the layer T near the Fermi surface.

Electron concentration n is a function of temperature in semiconductors. This function is determined by thermal ionization of impurities. It should be expanded in $T/\zeta \ll 1$ in the case of degenerate statistics:

$$n = n_0 + T\frac{dn}{dT}\bigg|_{T=0} . \tag{23}$$

The Fermi level E_F is well above the bottom of conduction band. It has a very weak temperature dependence[35] which we assumed to be negligible. Linear temperature dependence of the band gap E_g appears to be more significant. In order to take it into account in Eq. (23) one should count electron energy E in the equilibrium Fermi distribution function:

$$f_0 = \frac{1}{e^{\frac{E-E_f}{T}}+1} , \tag{24}$$

from the steady vacuum origin. Thus, we have

$$E = E_c + \frac{p^2}{2m^*} ,$$

where E_C denotes energy of the bottom of the conduction band. Thermal shift of E_C gives rise to linear temperature dependence of the chemical potential

$$\zeta = E_F - E_C , \tag{25}$$

which is counted from the bottom of the conduction band. The temperature derivative of the concentration n is expressed through a distribution function f_0 from Eq. (24) by means of identity

$$\frac{df_0}{dT} = \frac{1}{T}\left[\frac{p^2}{2m^*}-\zeta\right]\left[\frac{\delta f_0}{\delta\zeta}\right]_T + \left[\frac{\delta f_0}{\delta\zeta}\right]\frac{d\zeta}{dT} . \tag{26}$$

The second item of df_0/dT from Eq. (26) is nonvanishing at $T=0$ only. It gives after integration over the Brillouin zone:

$$\frac{dn}{dT}\bigg|_{T=0} = \frac{(2m^*)^{3/2}}{2\pi^2\hbar^3}\sqrt{\zeta}\frac{d\zeta}{dT}\bigg|_{T=0} . \tag{27}$$

The temperature derivative $d\zeta/dt\,/_{T=0}$ coincides with temperature shrinkage coefficient of the band gap:

$$\alpha = -\frac{dE_C}{dT}\bigg|_{T=0} = \frac{d\zeta}{dT}\bigg|_{T=0} . \tag{28}$$

Substitution of Eqs. (28), (27), and (23) into (22) and (21) gives

$$I_\sigma = \tfrac{3}{2}V\left[\frac{e^2}{mc^2}B_\sigma(\omega_I)\right]^2 |e_I \times e_s^*|^2 n\frac{T}{\zeta}\left[1+\frac{\alpha}{2}\frac{T}{\zeta}\right] . \tag{29}$$

There is a small parabolic correction to the usual linear temperature dependence in this equation.

The ratio of the cross sections in parallel and crossed polarizations of incident and scattered light equals[34]

$$\frac{I_\varepsilon}{I_\sigma} = \left[\frac{T}{\hbar\omega_I}\right]^2 D^2 , \tag{30}$$

where

$$D = \frac{\sum_j \frac{E_{gj}^2+(\hbar\omega_I)^2}{[E_{gj}^2-(\hbar\omega_I)^2]^2}\left[1+\frac{m_e^*}{m_j^*}\right]}{\frac{1}{E_g^2-(\hbar\omega_I)^2}-\frac{1}{(E_g+\Delta)^2-(\hbar\omega_I)^2}} . \tag{31}$$

V. NUMERICAL COMPARISON OF CALCULATED SCATTERING CROSS SECTIONS WITH EXPERIMENT

The theory of electronic light scattering, which is induced by different fluctuations of an electron gas in semiconductors with nonparabolic dispersion law of energy bands, described in the preceding section for a hydrodynamic free-electron-gas model, is applicable to the case of III-V compounds. We chose n-InP with $n = 1.1\times10^{18}$ cm^{-3}, which served as a well controlled model system. The experimental verification is obtained by the temperature dependent measurements of integrated cross sections and linewidths of quasielastic light-scattering spectra induced by different fluctuations of the electron gas in polarized and depolarized scattering configurations.

A. Temperature dependencies of integrated intensities of quasielastic light scattering from spin-, momentum-, and energy-density fluctuations

The estimation for n-InP and with $\hbar\omega_I = 1$, 17 eV, $E_g = 1$, 43 eV, $E_g+\Delta_0 = 1.54$ eV gives

$$D = \frac{25,77}{0.48} = 53.47; \quad \left[\frac{T}{\hbar\omega_I}\right]^2 = 3.88.10^{-4} , \tag{32}$$

and, thus,

$$\frac{I_\varepsilon}{I_\sigma} = 53.47^2\times3.88;10^{-4} = 1.11 . \tag{33}$$

So Eqs. (32) and (33) show that mechanisms of spin- and energy-density fluctuations give comparable intensities for the conditions of our experiments.

Theoretical temperature dependencies of the integrated intensities $I_{\varepsilon,p}$ and I_σ from Eqs. (20) and (29) are plotted in Fig. 3 by solid and dot-dashed lines, respectively, while filled and open circles represent corresponding experimental points. Adjustable parameters α and ζ equal $\alpha=4$, $\zeta=99$ meV. The dashed line represents a theoretical curve for $I_{\varepsilon,p}$,

$$I_{\varepsilon,p} = \left[\frac{e^2}{mc^2}\right]^2 [\xi B_p(\omega_i)]^2 V\left[\frac{\delta n}{\delta\zeta}\right]_T T\left[1+\frac{100T}{\zeta}\right] , \tag{34}$$

which is obtained using a temperature-independent clas-

sical value of the electron heat capacity

$$C_v = \tfrac{3}{2} k_B n \ , \tag{35}$$

k_B being the Boltzmann constant. It gives a poor fit to experimental points as compared with the solid line. The temperature dependence of C_v is, therefore, significant in accordance with the rather large value of $\zeta \gg T$. Before closing this section we would like to mention that our theoretical Eq. (33) and experimental findings (Figs. 1–3) demonstrate that there is no reason to neglect any of the above considered mechanisms of RS.

B. Temperature-dependencies of Lorentzian linewidths Γ

The decay of electron energy-density fluctuations occurs either via heat conductivity or via energy transfer to the host lattice of the crystal. The corresponding inverse time needed for the decay Γ_ε is the sum of two different contributions:

$$\Gamma_\varepsilon = q^2 \chi + \frac{1}{\tau_\varepsilon} \ , \tag{36}$$

where τ_ε is the electron temperature relaxation time, $\chi = x/C_v$, x is the heat conductivity, and χ is often referred to as heat diffusivity.[35,36] Relaxation time τ_ε has been calculated in Ref. 37 (Sec. 6.4). The appropriate result is

$$\frac{1}{\tau_\varepsilon} = \frac{2}{3} \frac{1}{\bar{\tau}} \left[\frac{\hbar\omega_0}{T} \right]^2 e^{-\frac{\hbar\omega_0}{T}} \ , \tag{37}$$

where $\hbar\omega_0$ is the energy of the low-frequency optical plasmon-phonon mode. It is equal for our n-InP, with $n = 1,\ 1.10^{18}$ cm^{-3}, $\omega_0 = 225$ cm^{-1},[22,34] $\bar{\tau}$ is the characteristic time of electron-phonon interaction. It is equal to $\tau = 0.14$ ps for n-GaAs,[37] which has related to n-InP electronic structure. To our knowledge this time is still unknown for n-InP today.[37] Its adjusted value which we obtain from our experimental results, plotted in Fig. 4 by filled circles is $\bar{\tau} = 0.06$ ps. Corresponding to Eq. (37) the theoretical curve is plotted in Fig. 4 by a dotted line.

The effect of the acoustic phonons on the linewidth Γ(36) is negligible. The Wiedemann-Franz law gives for quasielastic collisions

$$x = enuTL \ , \tag{38}$$

where μ is the mobility of electrons and L is the Lorentz number.

In the nondegenerate case it gives a pure diffusivity linewidth:

$$\Gamma_\varepsilon^\chi = \tfrac{2}{3} q^2 u \frac{T}{e} (r + \tfrac{5}{2}) \ , \tag{39}$$

where r is the power index in relaxation time-energy dependence $\tau \sim \varepsilon^r$. A straight-line plotted according to Eq. (39) fits well with the experimental points (filled circles).

Decay of the spin-density fluctuations also occurs via two different channels which are quite similar to the ones discussed above. The first of them demands two opposite diffusion current of electrons from different spin subbands. The contribution from the self-consistent electric field E, which is, in general, responsible for screening effects drops out from the relative diffusion current. It gives the inverse time for fluctuation decay:

$$\Gamma_\sigma = q^2 D \ , \tag{40}$$

where D is the diffusion coefficient. In the nondegenerate case this linewidth is also proportional to the temperature T:

$$\Gamma_\sigma = T q^2 \frac{\mu}{e} \tag{41}$$

The ratio of the straight line slopes plotted according to Eq. (39)—the upper one in Fig. 4—and to Eq. (41)—to the lowest one—gives the power index r:

$$\frac{\Gamma_\varepsilon^\chi}{\Gamma_\sigma} = \frac{2r+5}{3} \ . \tag{42}$$

A fitting procedure gives the following adjustable values $r = 0.435$ and $\mu = 1060$ cm^2/V sec. Electrical measurements give considerably higher values for $\mu = 2000$ cm^2/V sec (Ref. 34) and $\mu = 1720$ cm^2/V sec. Our adjusted value of r coincides with a mean of corresponding values listed in Ref. 35 [Eqs. (3.5a)–(3.5d)].

The second channel of spin-density fluctuation decay originates from spin splitting of the conduction band. It is discussed in a review paper[38] together with corresponding spin relaxation. The nonparabolic spin-orbit interaction used in the paper[38] has the form

$$H_{so} = \gamma_c [\sigma_x P_x (P_y^2 - P_z^2) + \sigma_y p_y (P_z^2 - P_x^2) + \sigma_z p_z (P_x^2 - P_y^2)] \ , \tag{43}$$

where γ_c is a phenomenological constant which equals 10 eV Å for n-InP according to Ref. 38. The spin-orbit interaction [Eq. (43)] is equivalent to the existence of an effective magnetic field in the crystal which is parallel to the unit vector entering Eq. (43):

$$x_x(p) = \frac{Px(P_y^2 - P_z^2)}{P^3}, \quad x_y(p) = \frac{P_y(P_z^2 - P_x^2)}{P^3} \ , \quad x_z(p) = \frac{Pz(P_x^2 - P_y^2)}{P^3} \ . \tag{44}$$

Therefore, the spin-quantization axis is not free. Its direction according to Eq. (42) depends on the direction of the electron quasimomentum. Thus, the spin-quantization axis changes in every collision.

It is shown in Ref. 39 that when the Raman shift ω is much smaller than the characteristic value of the spin-orbit splitting of the conduction band at the Fermi level $\Delta_{CF}(\omega \ll \Delta_{CF})$, the Lorentzian half-width Γ is equal

$$\Gamma = 1/\tau_{p_3} \ , \tag{45}$$

where τ_{p_3} is the relaxation time of the third Legandre polyminal. Theoretical estimation based on Hamiltonian (43) gives $\Delta_{CF} = 1$ meV for $n = 10^{19}$ cm^{-3} in InP. Our smallest value of $T_\sigma = 1.5$ meV $\geq \Delta_{CF}$. So we conclude

that in our experiments spin splitting is not important. Let us mention, however, that the opposite case $\Delta_{CF} \gg q^2 D$ can be achieved by using appropriate uniaxial stress which shifts the spin subbands with respect to each other.[38]

There is only one mechanism for the decay of momentum-density fluctuations (10) because momentum current

$$\Pi_{xy} \sim P_x p_y \ , \tag{46}$$

entering Eq. (10) is never conserved in a crystal with impurities. The corresponding Lorentzian half-width is determined in Refs. 40 and 41 to be equal to

$$\Gamma = 1/\tau_{p_2} \ , \tag{47}$$

where τ_{p_2} is the relaxation time of the second Legandre polynomial. Experimental determination of the half-width Eq. (47) in n-type materials demands more sensitive instrumentation and lower temperatures than we were able to obtain here.

VI. CONCLUSIONS

We have developed a hydrodynamical model for the free-electron gas in semiconductors with nonparabolic dispersion of energy bands under condition of frequent collisions and derived explicit expressions for electronic light-scattering cross sections. In our calculations, we considered different scattering mechanisms induced by spin-, energy-, and momentum-density fluctuations of the electron gas. This theory is applicable to the case of electronic light scattering in III-V semiconductors. We have demonstrated the first direct comparison with experimental results for temperature dependencies of the integrated intensities and spectral linewidths of electronic quasielastic light-scattering spectra. We found that various possible fluctuations of the electron gas were represented by different adequate line shapes with rather unusual discriminating polarized and depolarized scattering configurations and this gave us an opportunity to determine the corresponding relaxation times.

The experimental verification was performed on n-InP (with room-temperature dopant concentration $n = 1.1 \times 10^{18}$ cm^{-3}), which under the realization the condition of nonresonant near-infrared excitation with photon energies $\hbar\omega_i < E_g$, served as a well-controlled model system and enabled us to carry out reliable measurements in a wide temperature range 27–300 K. This situation is in contrast to the intensive electronic light-scattering studies that have been carried out recently with photon energies in resonance with spin-orbit split-off gaps or with quantum-well excitons. These measurements provided the required enhancement sensitivity, but, due to the simultaneous appearance of intense hot luminescence background, allowed one to carry out measurements only in a limited electron concentration range and prevented temperature-dependent measurements, which we have found are essential in order to reveal considerable controversy in the origin of different electronic fluctuations in semiconductors.

Finally, the theoretical approach to the problem and the observed experimental results provide clear evidence for the existence of strongly temperature-dependent free-electron-gas fluctuations in semiconductors with nonparabolic dispersion of energy bands and proves unambiguously the observation of light scattering from energy- and momentum-density fluctuations. This gives a sensitive measure of the magnitude of the different relaxation times of the electron gas.

ACKNOWLEDGMENTS

We are grateful to M. Cardona for valuable discussions and to B. P. Zakharchenya for supporting this work. One of the authors (B.H.B.) would like to thank the Science and Engineering Research Council for a Research Fellowship, R. T. Phillips for hospitality during his stay at the Cavendish Laboratory, and D. R. Richards for a critical reading of the manuscript.

*Present address: Department of Physics, Cavendish Laboratory, University of Cambridge, Madingley Road, Cambridge CB3 0HE, United Kingdom.

[1] E. Burnstein, M. Cardona, D. I. Lockwood, A. Pinczuk, and J. F. Young, in *Light Scattering in Semiconductor Structures and* Superlattices, Vol. 273 of *NATO Advanced Study Institute, Series B: Physics,* edited by D. J. Lockwood and J. F. Young (Plenum, New York, 1991), p. 1.

[2] A. Pinczuk and G. Abstreiter, in *Light Scattering in Solids V,* edited by M. Cardona and G. Guntherodt, Topics in Applied Physics Vol. 66 (Springer-Verlag, Berlin, 1989), p. 153.

[3] B. Kronast, H. Rohr, E. Glock, H. Zwicher, and E. Funfer, Phys. Rev. Lett. **16**, 1082 (1966).

[4] P. A. Wolf, Phys. Rev. **171**, 436 (1968).

[5] D. C. Hamilton and A. L. McWhorter, in *Proceeding of the International Conference on Light Scattering Spectra of Solids,* edited by G. B. Wright (Springer-Verlag, New York, 1969), p. 309.

[6] Y. Yafet, Phys. Rev. **152**, 855 (1966).

[7] A. Mooradian, Phys. Rev. Lett. **20**, 1102 (1968).

[8] R. J. Brueck, A. Mooradian, and F. A. Blum, Phys. Rev. B **7**, 5253 (1973).

[9] D. Olego, A. Pinczuk, and A. A. Ballman, Solid State Commun. **45**, 941 (1983)

[10] A. R. B. de Castro and R. S. Turtelli, Solid State Commun. **47**, 475 (1983).

[11] G. Abstreiter, M. Cardona, and A. Pinczuk, in *Light Scattering in Solids IV,* edited by M. Cardona and G. Guntherodt, Topics in Applied Physics Vol. 54 (Springer-Verlag, Berlin, 1984), p. 5.

[12] G. Fasol, N. Mesters, M. Dobers, A. Fischer, and K. Ploog, Phys. Rev. B **36**, 1565 (1987).

[13] M. Berz, J. F. Walker, P. von Allmen, E. F. Steigmeier, and F. K. Reinhart, Phys. Rev. B **42**, 11 957 (1990).

[14]D. Gammon, B. V. Shanabrook, J. C. Ryan, and D. S. Katzer, Phys. Rev. Lett. **68**, 1884 (1992).

[15]A. Pinczuk, B. S. Dennis, D. Heiman, C. Kallick, L. Brey, C. Tejedor, S. Schmitt-Rink, N. Pfeiffer, and K. W. West, Phys. Rev. Lett. **68**, 3623 (1992).

[16]B. Jusserand, D. Richards, H. Peric, and B. Etienne, Phys. Rev. Lett. **69**, 848 (1992); D. Richards, B. Jusserand, H. Peric, and E. Etienne (unpublished).

[17]A. Pinczuk, L. Brillson, E. Bernstein, and E. Anastassakis, Phys. Rev. Lett. **27**, 317 (1971).

[18]D. A. Abramson, K. T. Tsen, and R. Brey, Phys. Rev. B **26**, 6571 (1982).

[19]M. Cardona and G. Guntherodt, in *Light Scattering in Solids, VI,* edited by M. Cardona and G. Guntherodt, Topics in Applied Physics Vol. 68 (Springer-Verlag, Berlin, 1991), p. 1.

[20]U. Ekenberg, Phys. Rev. B **36**, 6152 (1987).

[21]M. Cardona and I. P. Ipatova (unpublished).

[22]B. H. Bairamov, I. P. Ipatova, V. A. Milorava, V. V. Toporov, K. Naukkarinen, T. Tuomi, G. Irmer, and J. Monecke, Phys. Rev. B **38**, 5722 (1988).

[23]G. Irmer, J. Monecke, B. H. Bairamov, and V. V. Toporov, Phys. Status Solidi C **136**, 481 (1986).

[24]B. H. Bairamov, Yu E. Kitaev, V. K. Negoduyko, and Z. M. Hashkhozev, Fiz. Tverd. Tela (Leningrad) **16**, 2036 (1974) [Sov. Phys. Solid State **16**, 1323 (1975)].

[25]B. H. Bairamov, I. P. Ipatova, V. V. Toporov, G. Irmer, J. Monecke, E. Jahne, K. Naukkarinen, and T. Tuomi, *Proceedings of the XVIIIth International Conference on the Physics of Semiconductors, Stockholm, 1986,* edited by O. Engström (World Scientific, Singapore, 1987), p. 1701.

[26]B. H. Bairamov, I. P. Ipatova, V. V. Toporov, and V. A. Voitenko, in *Proceedings of the Third International Conference on Phonon Physics,* edited by S. Hunklinger, W. Ludwig, and G. Weiss (World Scientific, Singapore, 1990), p. 793.

[27]M. Chandrasekhar, M. Cardona, and E. O. Kane, Phys. Rev. B **16**, 3579 (1977).

[28]L. D. Landau and E. M. Lifshitz, *Electrodynamics of Continuous Media* (Pergamon, Oxford, 1984).

[29]B. H. Bairamov, I. P. Ipatova, and V. A. Voitenko, Phys. Rep. **229**, 223 (1993).

[30]M. V. Klein, in *Light Scattering in Solids,* edited by M. Cardona, Topics in Applied Physics Vol. 8 (Springer-Verlag, Heidelberg, 1975), p. 146.

[31]L. D. Landau and E. M. Lifshitz, *Statistical Physics* (Pergamon, (Oxford, 1980), Parts I and II.

[32]V. A. Voitenko and I. P. Ipatova, Zh. Eksp. Teor. Fiz. **97**, 224 (1990) [Sov. Phys. JETP **70**, 125 (1990)].

[33]V. A. Voitenko, Fiz. Tverd. Tela (Leningrad) **29**, 3177 (1987) [Sov. Phys. Solid State **29**, 1827 (1987)].

[34]B. H. Bairamov, V. A. Voitenko, I. P. Ipatova, A. V. Subashiev, V. V. Toporov, and E. Jahne, Fiz. Tverd. Tela (Leningrad) **28**, 754 (1986) [Sov. Phys. Solid State **28**, 420 (1986)].

[35]A. I. Anselm, *Introduction to Semiconductor Theory* (Mir, Moscow, 1981).

[36]E. M. Lifshitz and L. P. Pitaevskii, *Physical Kinetics* (Pergamon, Oxford, 1981).

[37]V. F. Gantmarker and I. B. Levinson, *Carrier Scattering in Metals and Semiconductors* (Elsevier, North Holland, 1987).

[38]G. E. Pikus, V. A. Marushchak, and A. N. Titkov, Fiz. Tekh. Poluprovodn. **22**, 185 (1988) [Sov. Phys. Semicond. **22**, 115 (1988)].

[39]V. A. Voitenko, Fiz. Tverd. Tela (Leningrad) **33**, 3064 (1991) [Sov. Phys. Solid State **33**, 1730 (1991)].

[40]V. A. Voitenko, Fiz. Tverd. Tela (Leningrad) **98**, 3091 (1986) [Sov. Phys. Solid State **28**, 1739 (1986)].

[41]B. H. Bairamov, I. P. Ipatova, V. V. Toporov, and V. A. Voitenko, *Proceedings of the International Conference Held in Connection with the Celebration of Birth Century C. V. Raman and Diamond Jubilee of the Discovery of Raman Effect, Calcutta, 1988,* edited by C. P. Banerjee and S. S. Jha (World Scientific, Singapore, 1989), p. 386.